Time-resolved infrared-absorption study of photoinduced charge transfer in a polythiophene-methanofullerene composite film

Please check the document version of this publication:

• A submitted manuscript is the version of the article upon submission and before peer-review. There can be important differences between the submitted version and the official published version of record. People interested in the research are advised to contact the author for the final version of the publication, or visit the DOI to the publisher's website.
• The final author version and the galley proof are versions of the publication after peer review.
• The final published version features the final layout of the paper including the volume, issue and page numbers.
[Link to publication](link)

Time-resolved infrared-absorption study of photoinduced charge transfer in a polythiophene-methanofullerene composite film

S. C. J. Meskers, P. A. van Hal, and A. J. H. Spiering

Laboratory for Macromolecular and Organic Chemistry, Eindhoven University of Technology, P.O. Box 513,
5600 MB Eindhoven, The Netherlands

J. C. Hummelen

Stratingh Institute and MSC, University of Groningen, Nijenborgh 4, 9747 AG Groningen, The Netherlands

A. F. G. van der Meer

FOM Institute for Plasma Physics, P.O. Box 1207, 3430 BE Nieuwegein, The Netherlands

R. A. J. Janssen

Laboratory for Macromolecular and Organic Chemistry, Eindhoven University of Technology, P.O. Box 513,
5600 MB Eindhoven, The Netherlands

Photoinduced charge separation and recombination in poly(3-hexylthiophene)-fullerene derivative composite films is investigated at low temperature (80 K) by measuring the time-resolved photoinduced absorption due to the infrared active vibrational (IRAV) modes of the polymer in the region 1125–1300 cm^{-1}. The charge separation under 532 nm excitation (repetition rate 5 Hz) is found to be faster than the time resolution of the setup (<200 ps). The decay of charge carriers can be described with power-law kinetics $At^{-\alpha}$ with a single exponent $\alpha = 0.21$ from the subnanosecond to microsecond time scale. Hence, a large percentage of the charges created (80%) recombine within 30 ns, the remaining long-lived ones recombine on a millisecond time scale. On the millisecond time scale the decay can be approximated by a $1/t$ dependence. On the nanosecond time scale, the IRAV modes show only a small change in frequency upon varying the pump-probe delay, indicating that the polaronic charge carriers on the polymer do not undergo major relaxation processes in this time window.

Photoinduced charge transfer from π-conjugated polymers to C_{60} occurs on a subpicosecond time scale and with high efficiency.[1–4] The excess energy provided by the photoexcitation makes it possible to reach a metastable charge separated state in which an electron is transferred from the polymer to the C_{60}. Recombination of these charges was found to be a much slower process. The possibility to utilize the efficient photogeneration of long-lived charges in photovoltaic devices with a polymer-fullerene blend (bulk heterojunction) as the active layer has spurred further experimental research in this process.[5,6] The energy conversion of a bulk heterojunction photovoltaic device critically depends on the efficiency of charge carrier collection at the electrodes. For a high collection efficiency a bicontinuous morphology of the blend, high charge carrier mobilities, and a long lifetime of the charge-separated state are required. As a result of the ultrafast forward electron transfer reaction it has been proposed that charge separation occurs essentially with a quantum yield near unity.[1–4] For energy conversion, however, the fraction of charge carriers that escapes from (geminate) recombination is important. In this study we specifically address the lifetime of the charge-separated state, by studying the temporal evolution of photoinduced charge carriers from the subnanosecond to the millisecond time regime.

So far most experimental studies have relied on photoinduced absorption (PA) measurements in the visible and near-infrared spectral region to probe the charge carriers created. Overlap of photoinduced absorption bands of singlet and triplet (neutral) excitations on the polymer and on C_{60} with the absorption bands of the polaronic charge carriers makes it difficult to probe the charges specifically. However, in the infrared region, charged and neutral excitations can be more easily distinguished. While neutral excitations do not absorb significantly in this region, charged excitations on the conjugated polymer film give rise to strong infrared-active vibrations (IRAV) and these modes provide a unique probe for the net charge of the excitation.[7,8] Charge carriers on the π-conjugated chain are localized on a self-induced (local) distortion of the nuclear geometry of the polymer. Due to the structural distortion, the symmetrical Raman-active modes are converted into infrared-active modes giving rise to the IRAV bands.

PA measurements on conjugated polymer-fullerene blends in the infrared spectral region have provided direct spectral evidence for photoinduced charge transfer in these mixtures.[9,10] Most studies have relied on quasi-steady-state measurements, probing specifically long-lived charge carriers. Recently time-resolved measurements in the picosecond time range have appeared, employing IR probe pulses created by difference frequency mixing of short pulses from dye lasers.[11] This study showed that approximately 40% of the charge carriers generated in a poly(2-methoxy-5-(2'-ethylhexyloxy)-p-phenylene vinylene] (MEH-PPV)/C_{60} composite recombine in the first 600 ps after excitation. These results are qualitatively consistent with the subnanosecond decay observed in the near infrared (NIR) region.[3,4]
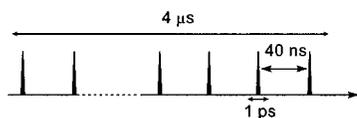
FIG. 1. Pulse structure of the FELIX macropulse consisting of a ~4 μs train of ~1 ps IR pulses, separated by 40 ns, at repetition frequency of 5 Hz.

In this paper we present time-resolved PA measurements using IR probe pulses from the free-electron laser FELIX in the Netherlands. FELIX emits tunable pulses with a remarkable pulse structure enabling one to follow the induced absorption from the subnanosecond into the microsecond time domain, a time span which is difficult to cover with a single more conventional IR probe source. The material studied is a blend of regioregular poly(3-hexylthiophene) (P3HT) and a derivative of C_{60}, 1-(3-methoxycarbonyl)-propyl-1-phenyl-[6,6]C_{61} ([6,6]PCBM).[12] The regioregular P3HT used in this study has a charge carrier mobility of $\sim 10^{-2}$ cm^2/V s when tested in a metal-insulator-semiconductor field-effect transistor (MISFET) configuration.[13,14] The modification of fullerene C_{60} to [6,6]PCBM allows larger amounts of fullerene to be mixed with the conjugated polymer without extensive phase segregation to occur but does not change the photoinduced electron transfer reaction significantly.[15]

As a pulsed infrared radiation source the free-electron laser, FELIX, at the FOM Institute for Plasma Physics in Nieuwegein, The Netherlands was used. The laser provides infrared pulses with approximately 1 ps duration and a spectral width in the region of interest of ~0.07 μm [full width at half maximum (FWHM)]. The actual output of the laser consists of a train of these ~1 ps pulses forming a macropulse with approximately 4 μs duration. The picosecond micropulses are separated by a 40 ns time interval. In Fig. 1 the pulse structure is illustrated. The repetition rate of the macropulses is 5 Hz. The output of a frequency doubled Nd:YAG laser (where YAG denotes yttrium aluminum garnet) (532 nm) was used to photoexcite the sample. The Nd:YAG laser was synchronized to the infrared source. Measurements were carried out at 80 K using an optical cryostat with ZnSe windows. The intensity of the transmitted infrared beam was measured with a Mercury Cadmium Telluride photodiode operating at room temperature. A long pass filter was placed directly in front of this diode to prevent the visible laser light from reaching the detector. The Nd:YAG pump and FELIX probe beams were combined in two different setups, one for probing the picosecond time regime and a one for probing PA in the nanosecond to microsecond regime.

To achieve picosecond time resolution the delay of the infrared probe pulse relative to the visible pump pulse was varied by means of an optical delay line. The output of the photodiode measuring the intensity of the transmitted infrared beam was integrated with a boxcar integrator. By modulating the visible light beam with an electronic shutter, successive light-on and light-off measurements were automatically subtracted by the boxcar integrator and the signal was averaged over seven on-off cycles. By scanning the optical delay line the rise of the photoinduced absorption could be recorded. The traces of five scans of the delay line were averaged to obtain the final signal. Recording also the

dark transmittance, the net change in absorption coefficient $\Delta A \cong -\Delta T/T$, where T is the transmittance and ΔT the change in transmittance due to photoexcitation by the pump, could be calculated.

To measure the photoinduced absorption in the nanosecond and microsecond time range, the output of the photodiode measuring the intensity of the transmitted infrared pulses was recorded in a time window from -1 to 3 μs relative to the pump pulse with a storage oscilloscope. The signal was averaged over typically 200 shots. Using an electronic shutter to modulate the excitation beam, the transmission with and without visible excitation could be recorded alternatingly in the following way. A second photodiode recording the visible pulse was positioned behind the electronic shutter and its output was used as a second trigger source for the storage oscilloscope alternative to the trigger signal from FELIX. The delay of the trigger signal from the photodiode relative to the trigger from the free-electron laser was adjusted electronically in such a way that it arrived approximately 8 ns earlier than the trigger from the free-electron laser (FEL). As the visible light pulses were periodically blocked by the electronic shutter, the oscilloscope was provided with the second alternative trigger signal for half of the shots from the Nd:YAG laser. In this way, the IR pulse train with visible light off appears in the oscilloscope trace with an apparent delay of 8 ns relative to the IR pulse train with visible light on. With a 300 MHz bandwidth for the detection, the signals did not overlap and could be integrated separately from the digitized oscilloscope trace.

To increase the time resolution beyond the 40 ns determined by the separation between the IR micropulses, the pulses were split by a ZnSe beam splitter and one part of the beam was sent through an optical delay line retarding the pulse by 20 ns and then recombined with the underlayed part. To further increase the time resolution beyond the 20 ns, the delay of the Nd:YAG pulse relative to the infrared micropulses was varied with steps of 2 ns over the 20 ns time interval.

Photoinduced absorption in the millisecond time range was measured between 0.25 and 3.5 eV by exciting with a mechanically modulated cw Ar-ion laser (528 nm) pump beam and monitoring the resulting change in transmission of a tungsten-halogen probe light through the sample (ΔT) with a phase sensitive lockin amplifier after dispersion by a triple grating monochromator and detection, using Si, InGaAs, and cooled InSb detectors. The pump power incident on the sample was typically 25 mW with a beam diameter of ~2 mm. Thin films were held at 80 K using an Oxford Optistat continuous flow cryostat.

Regioregular P3HT with molecular weight M_w $= 31$ kg/mol determined by size-exclusion chromatography (SEC) against polystyrene standards and polydispersity D $= 1.6$, was synthesized via the McCullough route[16] and purified with repeated Soxhlet extractions.[17] The regioregularity was determined to be 95% by ^{1}H NMR by comparing the signal intensities at 2.80 and 2.60 ppm. This procedure yields a lower but more reliable value than analysis of the aromatic region of the spectrum. [6,6]PCBM was synthesized according to previously published methods.[12] Amounts of P3HT and [6,6]PCBM, equal in weight, were dissolved separately
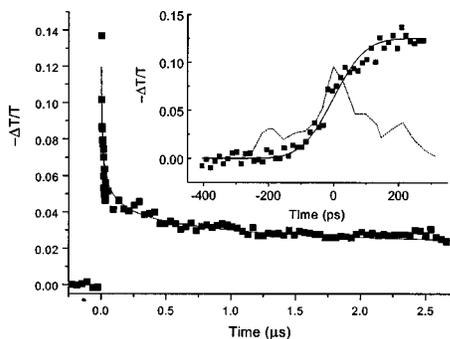
FIG. 2. Time dependence of the photoinduced absorption of the P3HT-[6,6]PCBM composite film monitored at 1275 cm^{-1} (7.87 mm) at 80 K. Excitation wavelength 532 nm, ~0.5 mJ/pulse, pump fluence ~2 mJ/cm^2. The solid line represents the fit of $A t^{-\alpha}$ with $\alpha = 0.21$ to the data. Inset: rise of the photoinduced absorption. The solid line is a fit of the error function to the data (see text) and the dashed line represents the autocorrelation of the pump pulse.

FIG. 3. Part of the photoinduced transient absorption spectrum of the P3HT-[6,6]PCBM composite film at 80 K. Pump: 532 nm, ~0.3 mJ/pulse and fluence ~0.3 mJ/cm^2. Filled squares: spectrum measured with 4 ns delay between pump and probe, open squares 60 ns delay.

in toluene (yielding solutions of 2% by weight) and then mixed. Films were made by drop casting the mixed solution on single-crystal NaCl plates.

In Fig. 2 the time dependence of the photoinduced absorption monitored at a single wavelength (1275 cm^{-1} or 7.87 μm) is shown. The inset shows the rise of the photoinduced infrared absorption together with the autocorrelation signal of the visible excitation pulse. A fit of the function $f(t) = A[1 - \text{erf}(t/\tau)]$, where erf is the error function, to the experimental signal is indicated by the solid line and a rise time τ of 0.11 ns was obtained. The fitted function corresponds to the signal expected for a long-lived photoinduced absorption created by an excitation pulse with a Gaussian temporal profile with 190 ps FWHM. The measured autocorrelation signal of the excitation pulse shows shoulders at ± 200 ps. From these measurements we conclude that the rise time of the photoinduced absorption is shorter than the time resolution of our instrument, and determined mainly by the temporal width of the visible excitation pulse. Thus the generation of charge carriers takes place on a time scale < 200 ps. This is in agreement with previous studies which suggest a subpicosecond photoinduced electron transfer.[2]

In the main part of Fig. 2 the decay of the photoinduced absorption following the rapid rise is illustrated. Within 25 ns the induced absorption is reduced to one-third of its maximum value, showing that a large part of the charges created recombines rapidly. About 20% of the polaronic charge carriers created survive the initial rapid recombination process and persist for at least several microseconds. The dynamics of the decay can be described by the function $R(t) = A t^{-\alpha}$, where $\alpha = 0.21 \pm 0.02$ for the subnanosecond to microsecond time span. The same type of decay of the photogenerated charge carriers, with a coefficient $\alpha = 0.07$, has been obtained in the 1–100 ps time regime for a composite of MEH-PPV and a similar C_{60} derivative in the NIR region.[4] Future experiments may show whether a simple power law suffices to describe the recombination kinetics in the entire 1 ps-1 μs time range in a conjugated polymer-fullerene blend.

The kinetics for charge recombination allow us to estimate the root-mean-square diffusion distance ($\bar{l}$) of the charge carriers in absence of an electric field from the rela-
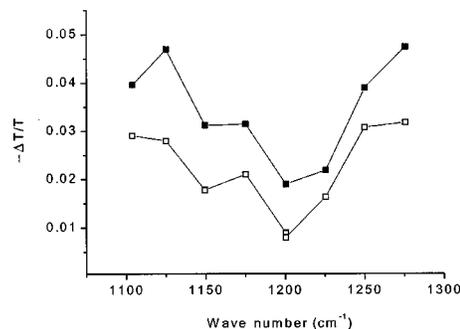
tion $\bar{l} = \sqrt{2Dt}$, where t is the time and D the diffusion constant given by the Einstein equation $D = \mu k T / e$ and, hence, depends on the charger carrier mobility. Taking $\mu \approx 10^{-2}$ cm^2/V s and $T = 300$ K, the time required to diffuse 100 nm (a typical layer thickness in a photovoltaic device) would be ~200 ns. Figure 2 shows that, even at 80 K where recombination is expected to be slower,[3] 70% of the charge carriers have recombined by this time. Of course these estimates change dramatically when the internal electric field of a photovoltaic device is taken into account. In that case the charges migrate under the influence of an electric field. A figure of merit for the time t to migrate a distance $l = 100$ nm under a 1 V potential difference (i.e., $E = 10^7$ V/m) would be $t = l/(\mu E) \approx 10$ ns. It is clear that by this time a significant amount (~50%) of recombination will have occurred.

The wavelength tunability of the FEL also allows for measurement of the infrared spectrum as a function of pump-probe delay. In Fig. 3 a small part of the infrared spectrum measured with a delay of 4 and 60 ns after excitation is shown. After 60 ns no further changes in the spectrum could be observed. The two main absorption bands at 1125 and 1275 cm^{-1} can be identified as the T_2 and T_4 modes, the shoulder at 1175 cm^{-1} with the far less intense T_3 mode. These T modes are attributed to uniform translational motion of the charged excitation along the polymer chain. Previously reported frequencies for these bands on P3HT detected using quasi-steady-state techniques are T_2, 1130; T_3, 1188; and T_4, 1269 cm^{-1};[18] in good agreement with our observations.

Earlier studies have revealed a considerable difference in infrared frequencies between the IRAV bands of photoinduced carriers and those induced by chemical doping,[9,10] suggesting that the IRAV frequencies are sensitive to the environment of the carrier. The present time-resolved study shows that minor changes in the IRAV spectrum occur with time indicating that the carriers do not undergo major relaxation processes in the time interval studied.

Finally, we have investigated the lifetime of the long-lived photogenerated polarons in the polymer-methanofullerene blend using a modulation technique with phase sensitive detection. Here the photoinduced absorption was measured at 3060 cm^{-1} (3.27 μm). By measuring the
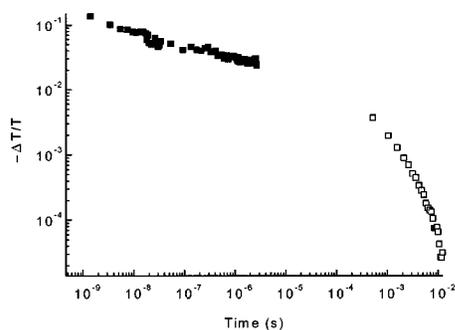
FIG. 4. Dependence of the photoinduced absorption signal on the pump-probe delay at 80 K. Solid squares: pump 532 nm, ~0.5 mJ/pulse, fluence ~2 mJ/cm^2, probe 7.87 mm from FEL. Open squares: Mechanically modulated continuous wave Ar$^+$ pump (25 mW) at 528 nm and probe at 3060 cm^{-1}. This latter signal has been corrected for the difference in absorption cross section at the two different probe wavelengths used.

dependence of the photoinduced absorption signal on the modulation frequency in the range from 30–4000 Hz and then doing a Fourier transformation on the data, the decay of the absorption signal in the millisecond time range can be determined. The resulting trace was corrected for the difference in the absorption cross section at 1275 and 3060 cm^{-1} and is shown in Fig. 4.[9] The data have not been corrected for the difference in the energy of the excitation pulses in the modulation and pump-probe experiment. Intensity and time dependence of the long-lived absorption indicate that the charge carriers disappear by recombination following bimolecular recombination kinetics.

Figure 4 illustrates that the recombination of photoinduced charge carriers takes place on multiple time scales spanning seven orders of magnitude. Recombination of the geminate charge pair created from a single excitation at the polymer C$_{60}$ interface is expected to make a major contribution to the rapid decay. The excess energy provided by the exothermic charge-transfer reaction is enough to allow for dissociation of the geminate pair into ''free'' charge carriers by a subsequent electron transfer step of the hole to a neighboring polymer chain or a jump of the electron between two fullerene molecules. These ''free'' charge carriers may then recombine with a charge carrier of opposite sign after diffu-

sional motion. In general, diffusion limited recombination processes in disordered materials follow complex kinetics with a time-dependent rate constant due to thermalization of the charge carriers and their trapping in the lowest states of the inhomogeneously broadened density of states. The decay may be described by a stretched exponential[19] or even more complex functions[20] and these equations can actually account for the difference in dynamic behavior in the two time domains studied in Fig. 4. The low mobility of the charge carriers in these organic materials compared to, e.g., inorganic semiconductors may then explain the longevity of the ''free'' carriers in comparison with those in inorganic materials.

We have shown that photoinduced charge carriers are generated in a forward electron transfer reaction with a rise time limited by the excitation pulse width (<200 ps). On the nanosecond time scale, the IRAV modes show only a small change in frequency upon varying the pump-probe delay, indicating that the polaronic charge carriers on the polymer do not undergo major relaxation processes in this time window. A large percentage (80%) of the charges created recombine within the first 30 ns after excitation; the remaining long-lived ones recombine on a millisecond time scale. The significant recombination of charge carriers at 30 ns may limit energy conversion that can be obtained with these composite materials in photovoltaic devices. Our experiments show that the decay of charge carriers follows a $At^{-\alpha}$ power law with $\alpha = 0.21$ from the subsnanosecond to the microsecond time scale. For related conjugated polymer-fullerene composites, similar kinetics have been observed in the 1–100 ps time regime[3,4] suggesting that charge recombination occurring in the ultrafast to intermediate time domain may perhaps be described by a single power law.

[1] N. S. Sariciftci et al., Science **258**, 1474 (1992).

[2] N. S. Sariciftci and A. J. Heeger, in *Handbook of Organic Conductive Molecules and Polymers*, edited by H. S. Nalwa (Wiley, New York, 1996).

[3] B. Kraabel et al., Phys. Rev. B **50**, 18 543 (1994).

[4] B. Kraabel et al., J. Chem. Phys. **104**, 4267 (1996).

[5] G. Yu et al., Science **270**, 1789 (1995).

[6] C. J. Brabec et al., Synth. Met. **102**, 861 (1999).

[7] B. Horovitz, Solid State Commun. **41**, 729 (1982).

[8] E. Ehrenfreund et al., Phys. Rev. B **36**, 1535 (1986).

[9] K. Lee et al., Phys. Rev. B **49**, 5781 (1994).

[10] H. Johansson et al., Synth. Met. **101**, 192 (1999).

[11] U. Mizrahi et al., Synth. Met. **102**, 1182 (1999).

[12] J. C. Hummelen et al., J. Org. Chem. **60**, 532 (1995).

[13] Z. Bao et al., Appl. Phys. Lett. **69**, 4108 (1996).

[14] H. Sirringhaus et al., Nature (London) **401**, 685 (1999).

[15] R. A. J. Janssen et al., J. Chem. Phys. **103**, 788 (1995).

[16] R. D. McCullough et al., J. Org. Chem. **59**, 904 (1993).

[17] M. Trznadel et al., Macromolecules **31**, 5051 (1998).

[18] Y. H. Kim et al., Phys. Rev. B **38**, 5490 (1988).

[19] J. C. Phillips, Rep. Prog. Phys. **59**, 1133 (1996).

[20] V. I. Arkhipov and H. Bässler, Philos. Mag. B **70**, 59 (1994).